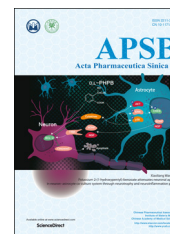




Chinese Pharmaceutical Association
Institute of Materia Medica, Chinese Academy of Medical Sciences

Acta Pharmaceutica Sinica B

www.elsevier.com/locate/apsb
www.sciencedirect.com



ORIGINAL ARTICLE

Identification and characterization of loop7 motif and its role in regulating biological function of human APOBEC3G through molecular modeling and biological assay



Congjie Zhai^a, Ling Ma^a, Zhixin Zhang^a, Jiwei Ding^a, Jing Wang^a,
Yongxin Zhang^a, Xiaoyu Li^a, Fei Guo^b, Liyan Yu^a, Jinming Zhou^{a,*},
Shan Cen^{a,*}

^aInstitute of Medicinal Biotechnology, Chinese Academy of Medical Science, Beijing 100050, China

^bInstitute of Pathogen Biology, Chinese Academy of Medical Science, Beijing 100050, China

Received 18 January 2017; received in revised form 19 April 2017; accepted 21 April 2017

KEY WORDS

HIV;
Vif;
APOBEC3G;
Motif;
Modeling;
hA3G–Vif complex;
hA3G dimer

Abstract Human APOBEC3G (hA3G) is a cytidine deaminase which inhibits HIV-1 replication. The HIV-1 accessory protein viral infectivity factor (Vif) counteracts with hA3G by targeting it for proteasomal degradation. In this work, we constructed and optimized molecular models of the hA3G dimer and the hA3G–Vif complex. The molecular modeling study revealed that the loop7 motif of hA3G appears on the interfaces of both the hA3G–Vif complex and the hA3G dimer. Biochemical analysis provided evidence suggesting that binding of Vif to hA3G results in steric blocking of hA3G dimerization, implying that monomeric hA3G serves as a substrate for Vif-mediated degradation. Furthermore, we presented evidence for the important roles of the loop7 motif, especially the central residues within the region, in hA3G dimerization, hA3G–Vif interaction, Vif-mediated hA3G degradation as well as subcellular localization of hA3G. This work highlights a multiple-task interface formed by loop7 motif, which regulates biological function of hA3G, thus providing the feasibility of the strategy of blocking Vif-mediated A3G degradation by targeting the putative site around loop7.

© 2017 Chinese Pharmaceutical Association and Institute of Materia Medica, Chinese Academy of Medical Sciences. Production and hosting by Elsevier B.V. This is an open access article under the CC BY-NC-ND license (<http://creativecommons.org/licenses/by-nc-nd/4.0/>).

*Corresponding authors. Tel./fax: +86 10 63037279.

E-mail addresses: zhoujinming@imb.pumc.edu.cn (Jinming Zhou), shancen@imb.pumc.edu.cn (Shan Cen).

Peer review under responsibility of Institute of Materia Medica, Chinese Academy of Medical Sciences and Chinese Pharmaceutical Association.

<http://dx.doi.org/10.1016/j.apsb.2017.05.002>

2211-3835 © 2017 Chinese Pharmaceutical Association and Institute of Materia Medica, Chinese Academy of Medical Sciences. Production and hosting by Elsevier B.V. This is an open access article under the CC BY-NC-ND license (<http://creativecommons.org/licenses/by-nc-nd/4.0/>).

1. Introduction

Human APOBEC3G (hA3G) is a member of the human APOBEC3 family of seven cytidine deaminases (A3A–A3H) that act as restriction factors of HIV. hA3G is incorporated into HIV-1 virions during virus assembly, and inhibits viral replication in the newly infected cells. Virion-encapsidated hA3G can deaminate cytosine to uracil on viral DNA during the reverse transcription of the viral genome, which leads to hypermutation of newly synthesized viral DNA^{1,2}. Furthermore, several lines of evidence showed that hA3G also impaired viral DNA synthesis and integration through a non-deaminating antiviral mechanism^{3–6}. As a counter measure, HIV-1 viral infectivity factor (Vif) binds to hA3G, and recruits a cellular ubiquitin ligase complex containing cullin 5 (CUL5), elongins B/C (ELOB/ELOC) and core-binding factor subunit β (CBF- β). This leads to the ubiquitination of hA3G and its degradation *via* proteasome-dependent degradation^{7–10}.

hA3G contains two tandem CMP/dCMP-type deaminase (CD) domains, the N-terminal (CD1) and the C-terminal (CD2). The C-terminal half of hA3G contains the catalytically active CD2 domain that is responsible for deaminase activity^{11,12}. The structure of the CD2 domain of hA3G has been determined by X-ray crystallography and NMR^{13–15}, the result of which shows that it folds into a five-stranded β sheet flanked by six α helices. While the CD1 domain is catalytically inactive, mutations in CD1 domain affect multiple aspects of hA3G function including dimerization, virion incorporation, subcellular distribution and interaction with Vif^{16,17}, suggesting that it is involved in virion encapsidation, and mediate oligomerization of hA3G^{18,19}. Unfortunately, there is, thus far, no CD1 domain structure determined by X-ray crystallography or NMR. Although different models have been proposed for the CD1 domain or for complete hA3G^{18–22}, the predicted structure and the structure–function relationships are still debated. In a recent model, the N- and C-terminal domains of a hA3G monomer are proposed to interact with each other *via* their β 2 strand, and the interaction is stabilized by RNA that binds to a cluster of positively charged residues at one edge of the head-to-head interface¹⁸. However, other studies proposed that the CD1 domains interact with each other as on the basis of the APO2 (A2) tetramer^{19,23}. Since it has been reported that the full structure of A2 in solution is a monomer, a tetrameric structure was thought to be unsuitable for the full-length structure and/or oligomer predictions of hA3G protein.

The crystal structure of Vif (PDB ID, 4N9F)²⁴, which binds to CBF- β and CUL5 E3 ligase complex, was recently solved. The solved structure should facilitate the understanding of how Vif interacts with hA3G. Several lines of evidence showed that the 122RLYYF WDP129 in hA3G plays a central role in its degradation by Vif. The D128 and P129 are known to be crucial for the binding of Vif to hA3G; however, the function of the 122–127 residues is less well understood. A recent report showed that all mutations that inhibit hA3G dimerization also inhibit the hA3G–Vif interaction. The authors also proposed that Vif either binds at the hA3G head-to-head interface or associates with an RNA-stabilized hA3G oligomer²³.

Although the functions of amino acids of hA3G and Vif have been studied intensively, their structure–function relationships remain poorly understood. To address this, we first constructed and optimized molecular models of the hA3G dimer and hA3G–Vif complex. Most of the predicted residues involved in the two complexes are consistent with published results of biochemical analysis, confirming accuracy and biological relevance of the predicted hA3G dimer and hA3G–Vif complex. The molecular modeling study reveals loop7 motif of hA3G appearing on the

interfaces of both hA3G–Vif complex and the hA3G dimer. Biochemical analysis provides evidence supporting the hypothesis that the monomeric hA3G may serve as a substrate for Vif-mediated degradation. Furthermore, we presented evidence for the important roles of loop7 motif, especially the central residues within the region, in hA3G dimerization, hA3G–Vif interaction, Vif-mediated hA3G degradation as well as subcellular localization of hA3G. This work highlights a multiple tasks interface formed by loop7 motif, which regulates cellular trafficking and biological function of hA3G. Finally, we propose that molecular modeling can serve as a guide for the further dissection of the structure–function relationships of domains and motifs within hA3G and Vif.

2. Materials and methods

2.1. Molecular modeling

The hA3G sequence (residues 1–384, Uniprot entry: Q9HC16, www.uniprot.org) was defined as the target sequence. The crystalized human A3F (PDB ID, 4J4J, www.pdb.org)²⁵ and the crystallized hA3G CD2 domain structure (PDB ID 3V4K)²⁶ served as the template of the NTD and CTD domain, respectively. The sequence alignment between target sequence and template sequence was performed using “Align Multiple Sequences” protocol in “Sequence Analysis” module of discover studio (DS), and the hA3G structure model was further built using “Build Homology Models” protocol in “Protein Modeling” module in DS. The homology model was evaluated through the “Profiles 3D” module in DS.

The hA3G–Vif complex and hA3G dimer were generated through protein–protein docking using the ZDOCK module and the initially obtained top-ranked poses were further optimized by RDOCK module in DS²⁷. ZDOCK uses a filtering feature to specify the residues involved in the binding interface and a blocking feature to specify the residues which certainly do not appear on the interface. The top 2000 poses were further evaluated through Z-RANK Score and clustered with the parameter of “RMSD_Cutoff” (10.0 Å) and “Interface_Cutoff” (10.0 Å). For the hA3G–Vif docking, we used the recently reported structure as the start structure of Vif. The residues D128–D130 of hA3G and the residues Y40–Y44 of Vif are specified for filtering^{17,28,29}, the residues D14–R17 and T74–W79 of Vif involved in A3F–Vif binding, which would not appear on the hA3G–Vif binding interface, are specified for blocking^{29,30}. For the hA3G–hA3G docking, the residues Y124–W127 of hA3G are specified for filtering during docking^{4,19,21}. In the refinement stage, RDOCK refinement was performed for the top 100 poses of the filtered ZDOCK output, and the poses were reranked using RDOCK scoring function. The CHARMM force field was applied for the proteins during RDOCK score calculation. The pose with lowest E_RDOCK score was selected as the binding mode of hA3G–Vif complex or the hA3G dimer. In addition, ionic interaction, hydrophobic, aromatic–aromatic and cation– π interactions between hA3G and Vif were analyzed employing protein interaction calculator (PIC, <http://crick.mbu.iisc.emet.in/~PIC>)³¹, the hydrogen bonds were analyzed in DS. The PDB files of the model structures to the manuscript is shown as [Supplementary information](#).

2.2. Cells and plasmids

293T cells were maintained in Dulbecco's modified Eagle's medium (DMEM) supplemented with 10% fetal bovine serum (FBS).

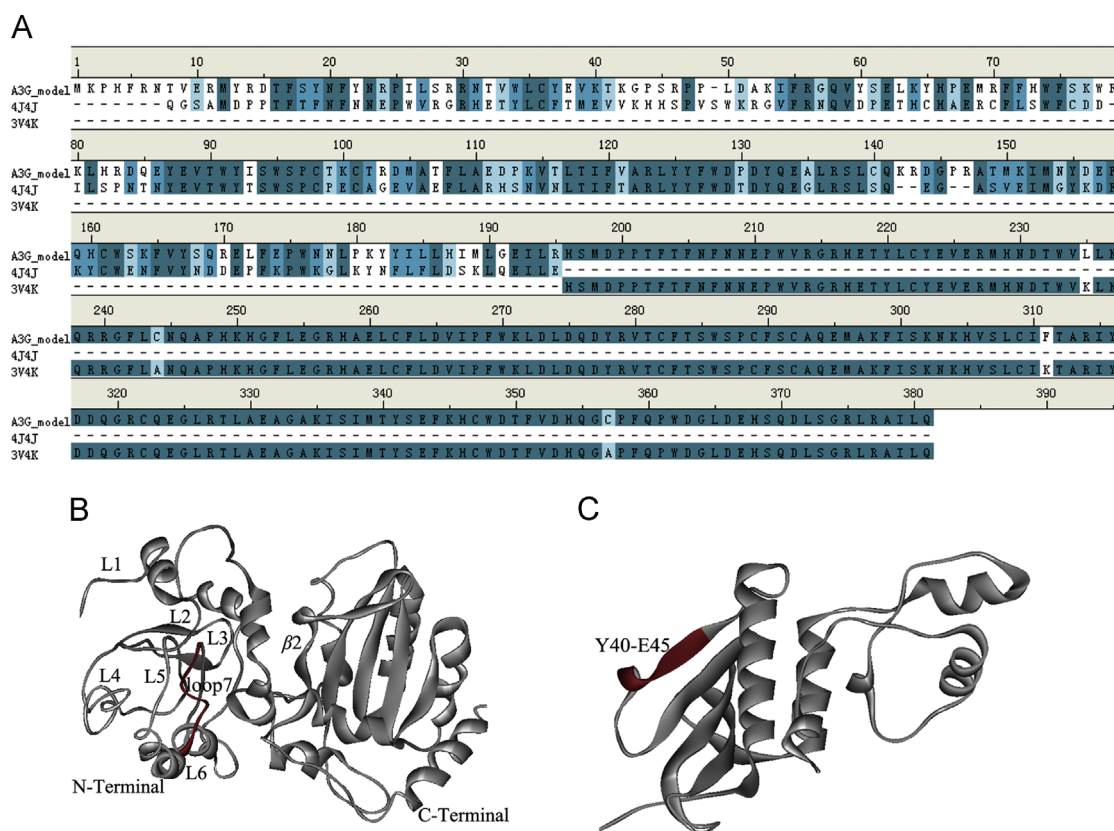


Figure 1 Molecule modeling of hA3G and Vif. (A) Sequence alignment between A3F and the CD1 domain of hA3G A3G NTD. (B) The predicted model of full-length A3G structure. The motif 122–129 was termed as “loop7” according to APOBEC3C structure (PDB ID: 3VOW), which is colored in red. (C) The crystal structure of Vif. The critical motif 40YRHHY44 are colored in red.

pcDNA-hA3G-HA has been described previously³². The cDNA fragment coding for hA3G amino acid was PCR-amplified and introduced a hemagglutinin (HA) tag at the C-terminus. In order to construct the amino acid substitutions of hA3G, QuikChange Lightning Site-Directed Mutagenesis Kit (Agilent Technologies, USA) was used to construct plasmid coding for hA3G containing mutation Y124A, Y125A, F126A, W127A, YY-AA, YYF-AAA, YYFW-AAAA, respectively, with either a HA tag or EYFP at the C-terminus of hA3G as indicated in Fig. 1. For BRET assay, two plasmids expressing fusion proteins, hA3G-EYFP and RLUC-hA3G, were generated by fusing Enhanced yellow fluorescent protein (EYFP) and renilla luciferase (RLUC) at C-terminal and N-terminal of hA3G, respectively.

2.3. Western blotting

293T cells were seeded at a density of 4×10^5 cells/well in 6-well plates 24 h prior to the transfection. The transfection was performed using Lipofectamine 2000 (Invitrogen, USA), according to the manufacturer's protocol. At 48 h post-transfection, cells were lysed in cell lysis buffer (Beyotime Biotechnology, USA) and subjected to SDS-PAGE analysis, followed by blotting onto PVDF membranes (Millipore, USA). Western blots were probed with specific antibodies designed to interact with Vif (2221, NIH AIDS Research and Reference Reagent Program, USA), HA-tag (Santa Cruz, USA), green fluorescent protein (GFP, Santa Cruz, USA), Myc (Sigma, USA) and β -actin (Abcam, USA). Detection of proteins was performed by enhanced chemiluminescence

(Millipore, USA). Bands in Western blots were quantitated using the Image LabTM 2.0 software automated digitizing system (Bio-rad, USA).

2.4. Fluorescence microscopy and fluorescence intensity assay

Hela cells were seeded on 20-mm glass bottom cell culture dishes (Nest, Switzerland) at a density of 5×10^4 cells/well. After 24 h of incubation, the cells were transfected with plasmids coding for hA3G wild type and mutants, respectively. After an additional 24 h of incubation, cells were fixed with 4% paraformaldehyde, permeabilized in 0.2% Triton X-100. Cells were washed with ice-cold PBS three times followed by addition of mounting medium with 4',6-diamidino-2-phenylindole (DAPI). Images of the live cells were captured on an Olympus FV1000 microscope (Olympus, Japan). Images were adjusted using FV10-ASW 3.0 software (Olympus, Japan). At 48 h post-transfection, cells were harvested and adjusted to 1×10^6 /mL. The 535 nm (± 10 nm) emitted light were determined with a VICTORTM X5 Multilabel Plate Reader (Perkin Elmer, USA).

2.5. BRET assay

The BRET assay used for detecting the protein–protein interaction as described previously³³. At 48 h post-transfection, cells were washed harvested and adjusted to 1×10^6 /mL. An aliquot of 1 μ L Coelenterazine-h (Promega, USA) was added into 100 μ L cells at a final concentration of 5 μ mol/L. The emitted light was determined

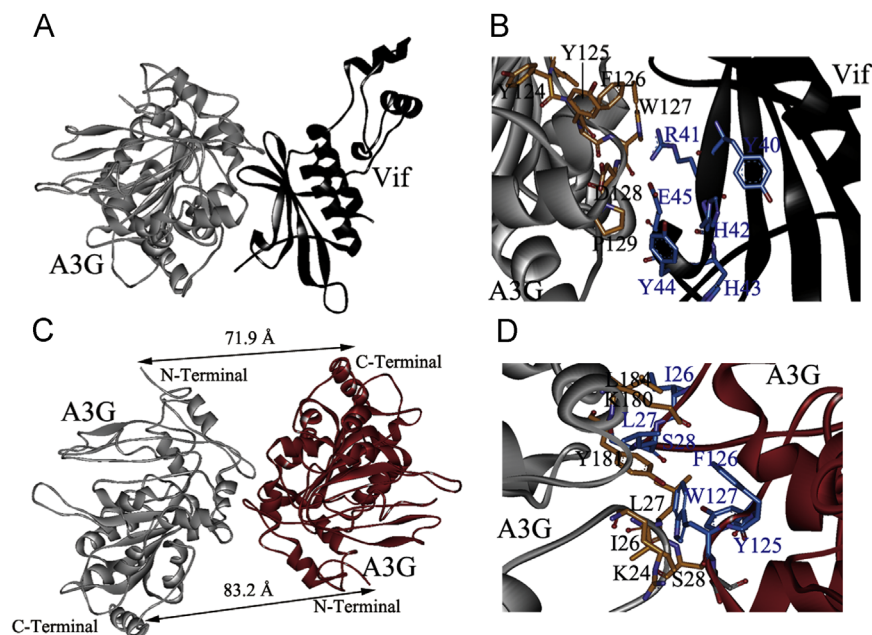


Figure 2 The predicted complexes of A3G/Vif and A3G/A3G. (A) The overall structure model of the A3G–Vif complex. (B) The crucial residues for interaction between Vif and A3G in the A3G/Vif predicted model. Loop residues 40YRHHY44 at Vif are in blue stick and loop7 residues at A3G in orange stick. (C) The overall structure model of the A3G–A3G complex. (D) The crucial residues for the interactions between A3G and A3G in the model of A3G dimer. Residues Y19, Y22, and W94 at one A3G monomer are in blue stick while loop7 residues (Y124, Y125, F126 and W127) at the other A3G monomer are in orange stick.

with a VICTOR X5 Multilabel Plate Reader. Readings at 475 nm (reflecting the bioluminescence given off by RLUC) and 530 nm (reflecting the resonance energy transfer from RLUC to EYFP) were measured simultaneously. The BRET ratio was calculated as emission at 530 nm (light emitted by EYFP)/emission at 475 nm (light emitted by RLUC). The BRET ratios reported were corrected by subtracting the ratios obtained in cells expressing the donor only (RLUC).

2.6. Co-immunoprecipitation

293T cells from 100-mm plates were collected at 48 h post-transfection and lysed in 500 μ L of NP-40 buffer (Beyotime Biotechnology, USA). Insoluble material was pelleted at 12,000 $\times g$ for 10 min at 4 $^{\circ}$ C. Protein was incubated with 5 μ L of anti-HA mouse antibody (Santa Cruz, USA) for 16 h at 4 $^{\circ}$ C, followed by the addition of protein A-Sepharose (Santa Cruz) for 2 h at 4 $^{\circ}$ C. The immunoprecipitate was then washed three times with ice-cold PBS. After the final supernatant was removed, 50 μ L of sample buffer (120 mmol/L Tris–HCl, pH 6.8, 20% glycerol, 4% SDS, 2% β -mercaptoethanol, and 0.02% bromophenol blue) was added, and the precipitate was then boiled for 10 min. After micro-centrifugation, the resulting supernatant was analyzed using Western blot.

3. Results

3.1. Molecular modeling

The homology model of full-length hA3G was constructed based on the templates of the crystallized human A3F (PDB ID, 4J4J) and the crystallized hA3G CD2 domain structure (PDB ID 3V4K).

Table 1 The interactions in the A3G/Vif model.

A3G-Vif interaction	Binding residues on the interface
Hydrophobic interaction	A3G:F126/W127/M188/L27-Vif:F39 A3G:P129-Vif:Y44 A3G:L184-Vif:P58
Ionic interaction	A3G:E191-Vif:K41 A3G:D128-Vif:E45 A3G:Y180-Vif:D61
Aromatic-aromatic interaction	A3G:F126/W127-Vif:F39
Hydrogen-bond interaction	A3G:W127-Vif:E45 A3G:G355-Vif:T47 A3G:Y180-Vif:G60 A3G:M188-Vif:K41 A3G:H345-Vif:K93

As the result of sequence alignment, the template A3F and the CD1 domain of hA3G have the high sequence identity of 41.5% with a sequence similarity of 57.9%, which means the template is suitable for homology model building (Fig. 2A). The CD1 domain of hA3G is composed by six helices and five β -sheets, which were linked by the loops. The motif 121–129 locates the seventh loop, thus we termed the motif as “loop7” (Fig. 2B). The structure of CD2 domain of hA3G is quite similar to its template structure (PDB ID 3V4K). It exhibits a discontinuous β 2-strand which is similar to its template structure (Fig. 2B). Particularly, the residues 128–130 of hA3G have been identified as essential for the interaction between Vif and A3G, as well as the series of residues, Tyr19, Tyr22, Trp94, Tyr124, Tyr125, Phe126, and Trp12723 in participation of the hA3G dimerization and its virion

incorporation, which were found at the protein surface and exposure to the solvent (Fig. 2B). Moreover, the Verify Score of the A3G structure (149.35) was close to the Verify Expected High Score (173.24), suggesting the high quality of the A3G structure model. The crystal structure of Vif, which binds to CBF- β and CUL5 E3 ligase complex, was recently solved, and we used the structure as the start structure of Vif. The Vif structure was extracted and shown in Fig. 2C. The critical residues (W38, 40YRHHY44, E45, and N48) for Vif/hA3G interaction were found at the protein surface and exposing to the solvent (Fig. 2C).

Based on the structures of hA3G and Vif, the hA3G-Vif complex was generated through protein-protein docking of hA3G and Vif model employing the ZDOCK and RDOCK program (Fig. 1A). The residues involved in the hA3G-Vif interaction were predicted by PIC and DS and listed in Table 1, most of which is consistent with the published results of biochemical analysis²³. This initially confirms the accuracy and biological relevance of the predicted hA3G-Vif complex. As shown in Fig. 1B, the hA3G-Vif interaction mainly involves loop7 motif (R122-P129) of hA3G and the Y40-E45 residues within Vif. The loop7 motif forms a hydrophobic groove on the hA3G surface, which is

flanked with several regions of negative charges. The Y40-E45 residues on the Vif are wedge-shaped, with the exposed loop region as front, narrow edge of the wedge. Notably, the motif 40YRHHY44 on Vif, a well-known region essential for binding to hA3G²⁸, is located in a groove surrounded by several hydrophobic and aromatic residues within the hA3G loop7 motif (Fig. 1B), such as F126, W127, and P29, resulting in a favorable hydrophobic and aromatic stacking interaction with the residues F39, R41 and Y44 of Vif. Also, the side chain of residues W127 and M188 of hA3G form hydrogen bonds with the residues E45 and K41 of Vif, respectively.

The model of hA3G dimer was also constructed using the ZDOCK and RDOCK program. As shown in Fig. 1C, two hA3G monomers form a dimer through two N-terminals in a head to head mode with a hydrophobic interface created by residues with loop7 motif. The residues involved in the hA3G dimerization were predicted by PIC and DS and listed in Table 2, most of which is consistent with the published results of biochemical analysis^{18,19,23}.

Comparing to previous reported results¹⁹ (constructed based on A2 tetramer through homology) the two A3G monomers in our dimer model are in similar mode. Particularly, the residues Y125, F126, W127, and M188 were found to be important for hA3G functionality in stabilizing the dimer (Table 2 and Fig. 1C) by forming numerous hydrophobic and π - π interactions between the hydrophobic and aromatic residues. These types of interactions are often found at protein-protein interfaces. Although the helix6, containing residues K180, Y181, L184, L185, and M188, is close to the putative dimer interface, the motif displays less extensive interactions with the other monomer than loop7 (Fig. 1D). Thus, from the model of hA3G dimer, loop7 residues play a crucial role for the formation of the A3G dimer.

3.2. Vif interrupts the formation of hA3G dimer

A close examination of the hA3G-Vif complex and the hA3G dimer (Fig. 3) reveals the loop7 motif of hA3G appearing on the interfaces of both complexes and overlapping binding sites shared by the two complexes. In agreement with this, residues F126 and W127 within loop7 were predicted to involve in both hA3G interaction with Vif and hA3G dimerization (Tables 1 and 2). This suggests that binding of Vif to hA3G results in steric blocking of

Table 2 The interactions in the A3G dimer model.

Interaction mode	Interaction residues on the interface
Hydrophobic interaction	R:P25-L:W127/L27
	R:I26-L:Y125/W127
	R:L27-L:Y125/W127
	R:Y181-L:L27/F126/W127/M188
	R:L184-L:P25/I26/L27
	R:L185-L:L27
	R:L188-L:I26
Ionic interaction	R:R29-L:D128
Aromatic-aromatic interaction	R:Y181-L:F126/W127
Cation- π interaction	R:K180-L:F126
Hydrogen-bond interaction	R:R24-L:W127
	R:S28-L:Y125
	R:N177-L:M188

R stands for the receptor A3G molecule.

L stands for ligand A3G molecule during protein-protein docking.

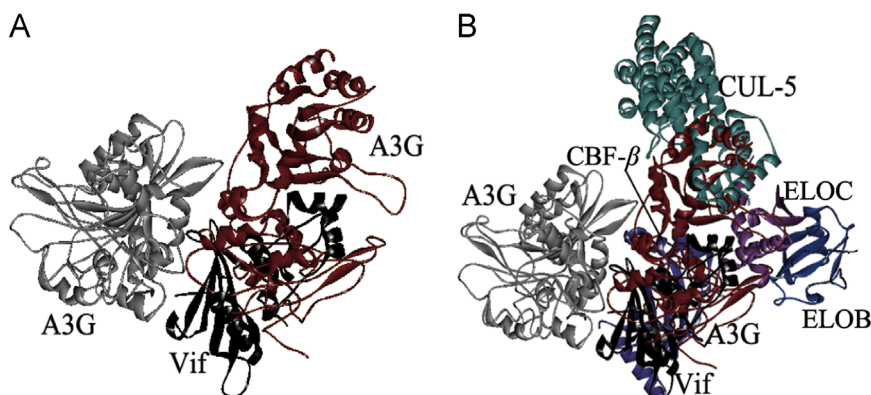


Figure 3 (A) The superimposition of A3G-Vif complex model and A3G dimer model. The A3G for superimposition is shown in grey ribbon, and Vif shown in black ribbon. The other monomer in A3G dimer is shown in red ribbon. (B) The superimposed structure is aligned with Vif/CUL-5/CBF- β /ELOC/ELOB complex. CUL-5 is shown in cyan ribbon. CBF- β is shown in purple ribbon. ELOC is shown in pink ribbon. ELOB is shown in blue ribbon.

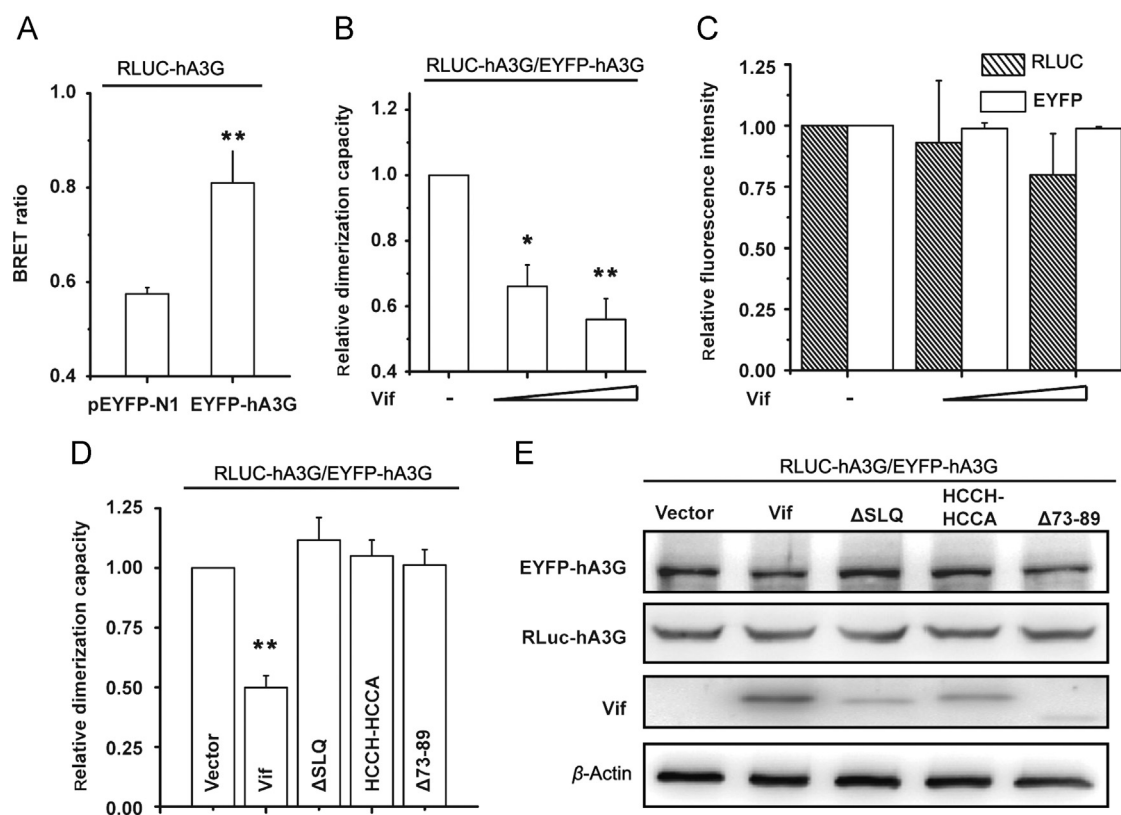


Figure 4 Vif interrupts the formation of hA3G dimer. 293T cells were co-transfected with plasmids as indicated. Fluorescence intensity measurement and Western blot analysis were performed 48 h post-transfection. (A) BRET analysis showed that hA3G formed dimeric states in cell. (B) In the presence of MG132, Vif still disrupted the dimer formation of hA3G, and in a dose-dependent manner. (C) Relative fluorescence intensity of panel B. (D) Detection of hA3G dimer formation in the presence of Vif and Vif mutants. (E) The cell lysates of panel D were probed with anti-GFP (top panel), anti-Vif (middle panel) and anti- β -actin (bottom panel) antibodies. * $P \leq 0.05$, ** $P \leq 0.01$, *** $P \leq 0.001$ (\pm SD).

the interaction between two hA3Gs, leading to a hypothesis that HIV-1 Vif could interrupt the formation of hA3G dimer. Indeed, when superimposing the hA3G-Vif complex and the hA3G dimer, a crash occurred due to overlap between the Vif interaction site and the hA3G head-to-head interface (Fig. 3A). Since it is known that Vif will recruit CBF- β and CUL5 E3 ligase complex when it downregulates A3G, we aligned the Vif complex to the superimposed structure. It indicated that the A3G dimer does not only have a crash with Vif, but also has crash with CUL5 and ELOB (Fig. 3B).

To further examine this hypothesis, we first utilized a bioluminescence resonance energy transfer (BRET) assay to assess the effect of Vif upon hA3G dimerization. In this assay, two plasmids expressing fusion proteins hA3G-EYFP and hA3G-RLUC were generated by fusing EYFP and *Renilla* luciferase at C-terminal and N-terminal of hA3G, respectively. Upon heterodimerization of two fusion proteins, resonance energy transfer can occur between RLUC/EYFP fusion proteins that interact, resulting in a BRET ratio that quantitatively reflects the interaction between the two hA3Gs. Compared with the co-transfection with the EYFP empty vector, the BRET ratio was significantly increased when the cells were co-transfected with EYFP-hA3G (Fig. 4A), indicating that the BRET assay is suitable for assessing hA3G dimerization in cell.

To investigate whether Vif interrupts hA3G dimer formation, 293T cells were co-transfected with plasmids coding for RLUC-hA3G, EYFP-hA3G and Vif in the presence of a proteasome inhibitor MG132. MG132 was shown to inhibit Vif-mediated degradation of hA3G but not the hA3G/Vif interaction³⁴. As shown

in Fig. 4B, the expression of Vif reduced the BRET ratio produced by hA3G heterodimers in a dose-dependent manner, suggesting that Vif inhibits the dimerization of hA3G in cell. Next, the lysate of the transfected cells were subjected to fluorescence density measurement (Fig. 4C) and Western blot analysis (data not shown) so as to determine if the expression of fusion proteins varied under the experiment condition, which might cause a reduction in hA3G dimerization as well as BRET ratios. The results show no significant change in the expression of hA3G, indicating that the presence of Vif results in reduced hA3G dimerization, regardless of the degradation of hA3G by Vif (Fig. 4C). Taken together, these data suggest that binding of Vif to hA3G results in steric blocking of hA3G dimerization, and monomeric hA3G may serve as a substrate for Vif-mediated degradation.

Vif acts as an adaptor to interact with cellular CUL5, ELOB/C and CBF- β , resulting in the formation of E3 ubiquitin ligase complex and consequently binds hA3G³⁵⁻³⁸. It is of interest to understand if the components other than Vif in the E3 ligase complex contribute to Vif inhibition of hA3G dimerization. Thus, we transfected a series of plasmids coding Vif mutants into 293T cells, and assessed their effect upon the dimer formation of hA3G. It is known that Vif Δ SLQ and Vif HCCH-HCCA lost their abilities to interact with ELOC and CUL5, respectively^{36,38-40}. We assessed the dimer formation of hA3G in the presence of either one of the two Vif mutants using the BRET assay described above, and found that neither was active as wild type Vif did in cell (Fig. 4D), while cellular contents of all Vif mutants were similar to that of wild type Vif (Fig. 4E). It suggests that the formation of the

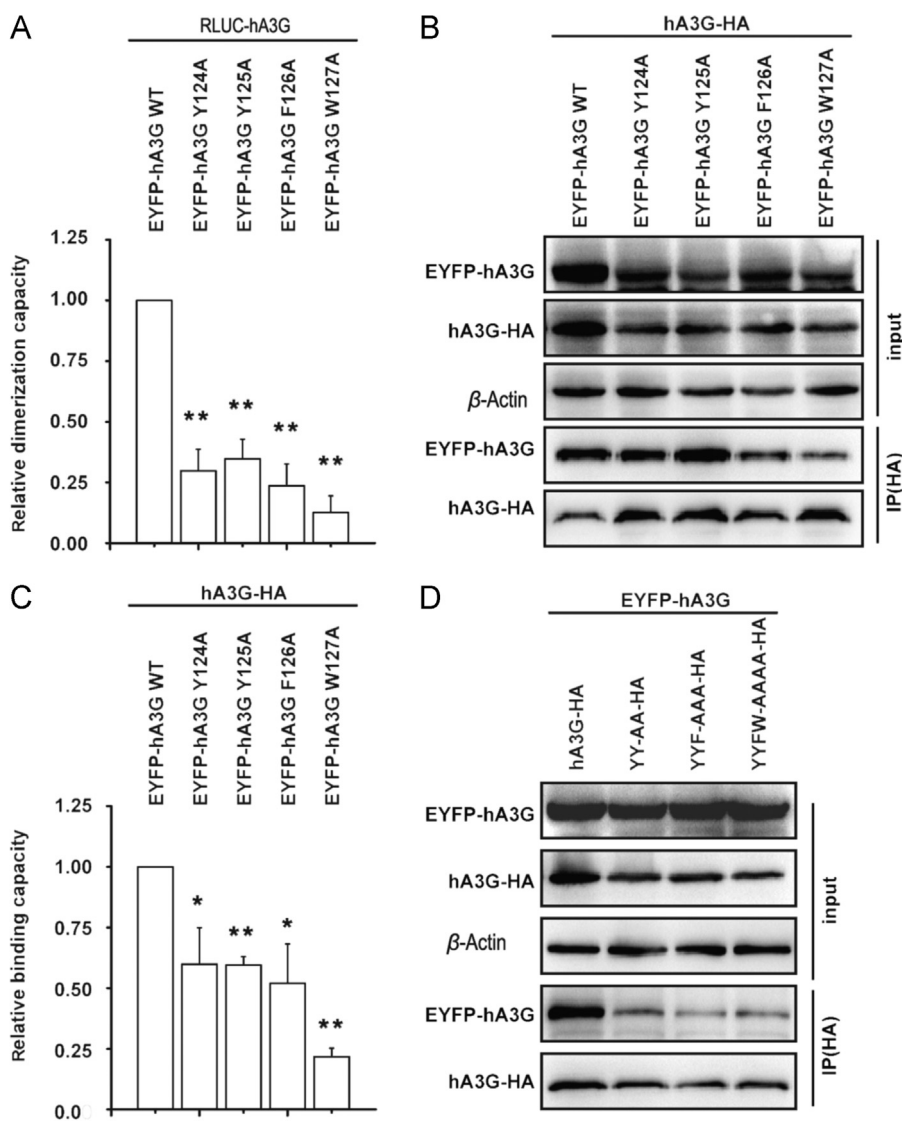


Figure 5 The critical amino acids in loop7 play an important role in hA3G dimer formation. 293T cells were co-transfected with plasmids as indicated. Fluorescence intensity measurement and Western blot analysis were performed 48 h post-transfection. (A) Single amino acid substitutions in loop7 of hA3G disrupted the dimer formation. (B) Western blots of cell lysates (input) from panel A were probed with anti-GFP (top panel), anti-HA (middle panel) and anti- β -actin (bottom panel) antibodies, respectively, or anti-HA immunoprecipitates (IP) from cell lysates were probed with anti-GFP (upper panel) and anti-HA (lower panel) antibodies. (C) Quantitative analysis of panel B, immunoprecipitates. Image LabTM 2.0 software was used for calculation. (D) Multiple amino acid substitutions in loop7 of hA3G enhanced the interruption of hA3G-hA3G binding. Western blots of cell lysates (input) were probed with anti-GFP (top panel), anti-HA (middle panel) and anti- β -actin (bottom panel) antibodies, respectively, or anti-HA immunoprecipitates (IP) from cell lysates were probed with anti-GFP (upper panel) and anti-HA (lower panel) antibodies. * $P \leq 0.05$, ** $P \leq 0.01$, *** $P \leq 0.001$ (\pm SD).

E3 ligase complex may be a prerequisite for Vif-mediated inhibition on hA3G dimerization. As expected, Vif $\Delta 73-89$ that is unable to interact with hA3G^{41,42} shows loss of its ability to disrupt hA3G dimer (Fig. 4D).

3.3. The central residues on loop7 motif of hA3G mediate hA3G dimerization

The central residues (Y124-W127) on loop7 motif of hA3G appear on both hA3G-Vif and hA3G-hA3G interfaces (Fig. 2), which are also predicted to mediate these two interactions

(Tables 1 and 2). To further validate the functions of loop7 motif, we first utilized the BRET assay to investigate the roles of the central residues on loop7 in hA3G dimerization using single amino acid substitution mutants of loop7, *i.e.*, Y124A, Y125A, F126A and W127A. Compared with hA3G homodimer, the heterodimer complex between each of the four mutants and hA3G was reduced by more than 70%–85% (Fig. 5A), suggesting that the central residues on loop7 indeed facilitate the dimerization of hA3G. To better define the underlying mechanism, we further assessed the ability of the four mutants to interact with hA3G using a co-immunoprecipitation (Co-IP) assay (Fig. 5B). Similar to the result of the BRET assay, Co-IP analysis showed that the substitution

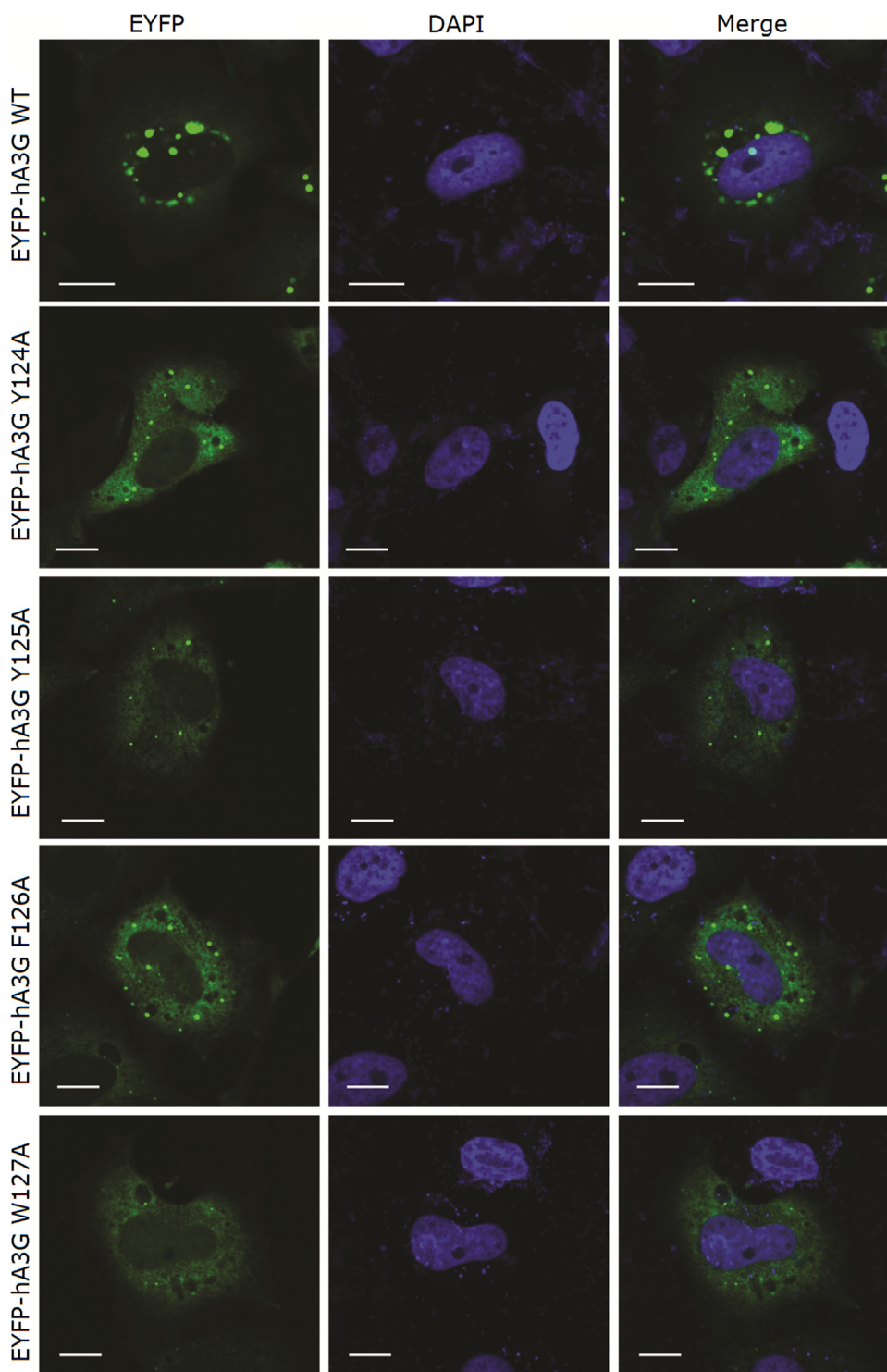


Figure 6 Single amino acid substitutions in loop7 of hA3G disrupt cytoplasmic localization. Representative images of HeLa cells transfected with the indicated pEYFP-hA3G wild type and mutant expression plasmids were shown. The EYFP-tagged constructs were visualized in fixed cells. Scale bar: 10 μ m.

mutations of loop7 impair their abilities to bind to hA3G (Fig. 5C). Accordingly, the multiple amino acid substitutions of this region caused more reduction in hA3G dimer compared with hA3G–Y124A (Fig. 5D), suggesting that these residues synergically facilitate hA3G dimerization.

It should be worthy of note that W127A inhibits binding of mutated hA3G to wild type by approximate 80%, while inhibitory

effect of other mutants show less than 50% (Fig. 5C) to a lesser extent than that found in the BRET assay (Fig. 5A). Despite that many factors, such as sensitivity of experimental approach, may account for the different results found in the two assays. This raises a possibility that the mutated loop7 alters subcellular localization of hA3G, resulting in additional inhibition on its interaction with wild-type hA3G in living cells. In support of this, previous studies have

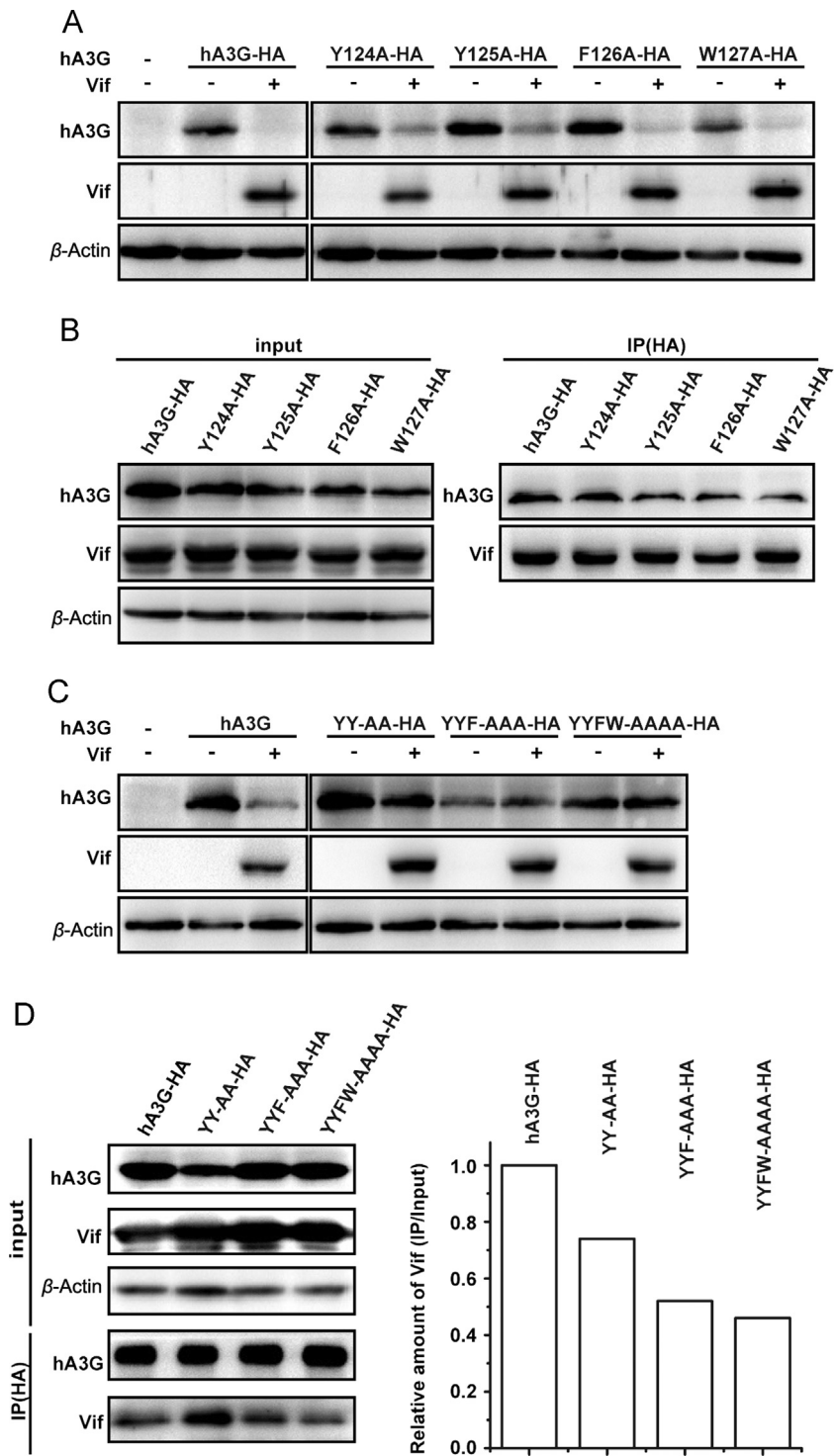


Figure 7 The ability of critical amino acid in loop7 of hA3G to be degraded by Vif and bind to Vif. 293 T cells were co-transfected with plasmids as indicated. (A) Western blots of cell lysates were probed with anti-HA (top panel), anti-Vif (middle panel) and anti- β -actin (bottom panel) antibodies, respectively. (B) Effects of single amino acid substitutions in loop7 of hA3G on binding to Vif. Western blots of cell lysates (input) were probed with anti-HA (top panel), anti-Vif (middle panel) and anti- β -actin (bottom panel) antibodies, respectively, or anti-HA immunoprecipitates (IP) from cell lysates were probed with anti-HA (upper panel) and anti-Vif (lower panel) antibodies. (C) Western blots of cell lysates were probed with anti-HA (top panel), anti-Vif (middle panel) and anti- β -actin (bottom panel) antibodies, respectively. (D) Left panel: Effects of multiple amino acid substitutions in loop7 of hA3G on binding to Vif. Western blots of cell lysates (input) were probed with anti-HA, anti-Vif and anti- β -actin antibodies, respectively, or anti-HA immunoprecipitates (IP) from cell lysates were probed with anti-HA and anti-Vif antibodies. Right panel: Vif in cell lysate and immunoprecipitates were quantified using Image LabTM 2.0 software. The ratio of Vif in immunoprecipitates to cell lysate were calculated and normalized to that of wild type Vif. * $P \leq 0.05$, ** $P \leq 0.01$, *** $P \leq 0.001$ (\pm SD).

reported that hA3G localizes to mRNA processing bodies (PBs) and two regions of hA3G N-terminal half involved in cytoplasmic localization^{43–45}. Indeed, the fluorescence microscope analysis revealed that hA3G localized throughout the cytoplasm and mainly formed cytoplasmic foci (Fig. 6) similar to the previous report⁴³. Like wild type hA3G, four loop7 mutants, including Y124A, Y125A, F126A and W127A, remained cytoplasmic localization. However, these four mutants, especially Y125A and W127, exhibited impaired abilities to form cytoplasmic foci and were spread throughout the cytoplasm (Fig. 6). The results suggest that the central residues (Y124–W127) on loop7 motif of hA3G play an important role in its subcellular localization, and that altered subcellular localization of loop7 mutants contributes to their inhibitory effect on hA3G dimerization in cell.

3.4. Role of the central residues on loop7 motif of hA3G in hA3G–Vif interaction

Modeling analysis revealed that the central residues (Y124–W127) on loop7 motif of hA3G also interact with Vif. Therefore, we used the single amino acid substitution mutants mentioned above to verify the prediction. First, we investigated the sensitivities of these mutants to Vif-mediated degradation, and found that Vif is able to reduce the cellular content of hA3G mutants as well as wild type hA3G (Fig. 7A). Accordingly, Co-IP analysis showed that these mutants only cause slight decrease in their abilities to bind with Vif (Fig. 7B). All these results suggest that single amino acid substitution of the central residues on loop7 motif may be insufficient for interrupting the hA3G–Vif interaction. Thus, we further examined the effect of multiple amino acid substitutions of loop7 on Vif-mediated hA3G degradation and the hA3G–Vif interaction. In contrast to the results from the single amino acid substitutions, the results with multiple amino acid substitutions resulted in resistance to Vif (Fig. 7C). Co-IP results revealed that these hA3G mutants exhibited reduced ability to bind Vif compared with wild type hA3G, and the interaction between Vif and hA3G became weaker along with increased number of amino acid substitution (Fig. 7D). These results suggest that the predicted interaction plays an important role in binding of hA3G to Vif. In agreement with our result, a recent work reported that mutations of residues 122 RLYYFW 127 were found to inhibit Vif–hA3G interaction using mammalian protein–protein interaction trap (MAPPIT) in cell two-hybrid system²³.

4. Discussion

In this work, we established and optimized molecular models of full length hA3G and HIV-1 Vif, and then constructed the hA3G dimer and hA3G–Vif complex *via* protein–protein docking (Fig. 2). Most of predicted residues involved in the two complexes are consistent with published results of biochemical analysis, confirming accuracy and biological relevance of the predicted hA3G dimer and hA3G–Vif complex. We thus propose that these molecular modeling can serve as a guide for the further dissection of the structure–function relationships of domains and motifs within hA3G and Vif. Furthermore, structure analysis and function validation in this work have presented evidence for the important roles of loop7 motif in hA3G dimerization, hA3G–Vif interaction, Vif-mediated hA3G degradation, as well as subcellular localization of hA3G. Interestingly, our previous work predicted a binding site close to loop7. The multiple-task interface formed by loop7 motif

indicates the feasibility of the strategy targeting the putative site to block Vif-mediated A3G degradation.

Although the mechanism of hA3G degradation by Vif has been extensively studied, it remains largely unclear how Vif interacts with hA3G. The molecular modeling study presented herein reveals loop7 motif of hA3G appearing on the interfaces of both hA3G–Vif complex and hA3G dimer, and overlapping binding sites shared by the two complexes (Fig. 3), suggesting that Vif may interrupt the formation of hA3G dimer. Indeed, the biochemical analysis in this work provides evidence supporting that binding of Vif to hA3G results in steric blocking of hA3G dimerization (Fig. 4). These results lead to a hypothesis that monomeric hA3G may serve as a substrate for Vif-mediated degradation. Despite difficulty in obtaining direct experimental evidence, *i.e.*, hA3G dimer is resistant to Vif, this hypothesis is supported, at least in part, by the several previous works showing that the oligomerization-defective hA3G mutants were efficiently degraded by Vif^{19,46}. In addition, our data showed that binding of Vif to hA3G is necessary, but not sufficient, for blocking hA3G dimerization, and that forming a Vif containing E3 ligase complex is further required (Fig. 4). This is consistent with an early observation that Vif C133S did not interfere with hA3G oligomerization, in spite of associating with hA3G but not CUL5¹⁹. The explanations for the observation include that binding of Vif alone is insufficient for forming a steric blockage. However, the precise contribution of Vif–CUL5–SCF (SKP1–CUL–F-box) complex to the inhibition to hA3G dimerization must await advances in the biochemical characterization of its interaction with hA3G.

Several lines of evidence showed that the 122RLYYFWDP129 in hA3G play a central role in its degradation by Vif. The D128 and P129 are known to be crucial for binding of Vif to hA3G; however, the function of the 122–127 residues is much less understood. Our molecular modeling predicts an interaction of Vif and the central residues (124YYFW127) on the loop7 (Figs. 2 and 3). Accordingly, mutagenesis analysis presented herein revealed that the predicted interaction involving the central residues on loop7 motif plays an important role in Vif-mediated hA3G degradation (Fig. 7). Consistent with our result, Gooch and Cullen⁴⁷ reported that the replacement of 124YYFW127 in hA3G with the corresponding hA3A sequence abolished the sensitivity of hA3G to Vif, and a converse mutation in hA3A turns it into a target for Vif-mediated degradation.

In summary, our structure and function analysis has presented evidence for the important roles of loop7 motif in hA3G dimerization, hA3G–Vif interaction, Vif-mediated hA3G degradation as well as subcellular localization of hA3G. Together with previous studies, this work highlights a multiple-task interface formed by loop7 motif, especially the central residues within the region, which mediates interactions of hA3G with viral and host proteins and regulates cellular trafficking and biological function of hA3G. Ultimately, this work may help endeavors aimed at therapeutic intervention with the interaction between the HIV-1 Vif protein and hA3G.

Acknowledgements

The authors thank National Infrastructure of Microbial Resources (NIMR-2014-3) for providing valuable reagents. This work was supported by 973 program (2012CB911102 CS), National Mega-project for Innovative Drugs (2012ZX09301002-001-015 and 2012ZX09301002-005-002 CS), National Mega-Project for Infectious

Disease (2013ZX1000 4601-002 CS), and The National Natural Science Foundation of China (81271844 ZJM and 31470272 CS). Shan Cen and Jinming Zhou are supported by Xiehe Scholar.

Appendix A. Supplementary material

Supplementary data associated with this article can be found in the online version at <http://dx.doi.org/10.1016/j.apsb.2017.05.002>.

References

- Zhang H, Yang B, Pomerantz RJ, Zhang C, Arunachalam SC, Gao L. The cytidine deaminase CEM15 induces hypermutation in newly synthesized HIV-1 DNA. *Nature* 2003;**424**:94–8.
- Yu Q, König R, Pillai S, Chiles K, Kearney M, Palmer S, et al. Single-strand specificity of APOBEC3G accounts for minus-strand deamination of the HIV genome. *Nat Struct Mol Biol* 2004;**11**:435–42.
- Li XY, Guo F, Zhang L, Kleiman L, Cen S. APOBEC3G inhibits DNA strand transfer during HIV-1 reverse transcription. *J Biol Chem* 2007;**282**:32065–74.
- Iwatani Y, Chan DS, Wang F, Maynard KS, Sugiura W, Gronenborn AM, et al. Deaminase-independent inhibition of HIV-1 reverse transcription by APOBEC3G. *Nucl Acids Res* 2007;**35**:7096–108.
- Guo F, Cen S, Niu MJ, Saadatmand J, Kleiman L. The inhibition of tRNA^{Lys3}-primed reverse transcription by human APOBEC3G during HIV-1 replication. *J Virol* 2006;**80**:11710–22.
- Guo F, Cen S, Niu MJ, Yang YL, Gorelick RJ, Kleiman L. The interaction of APOBEC3G with human immunodeficiency virus type 1 nucleocapsid inhibits tRNA^{Lys3} annealing to viral RNA. *J Virol* 2007;**81**:11322–31.
- Ebrahimi D, Anwar F, Davenport MP. APOBEC3G and APOBEC3F rarely co-mutate the same HIV genome. *Retrovirology* 2012;**9**:113.
- Dang Y, Davis RW, York IA, Zheng YH. Identification of ⁸¹LGxGxxIxW⁸⁹ and ¹⁷¹EDRW¹⁷⁴ domains from human immunodeficiency virus type 1 Vif that regulate APOBEC3G and APOBEC3F neutralizing activity. *J Virol* 2010;**84**:5741–50.
- Russell RA, Smith J, Barr R, Bhattacharyya D, Pathak VK. Distinct domains within APOBEC3G and APOBEC3F interact with separate regions of human immunodeficiency virus type 1 Vif. *J Virol* 2009;**83**:1992–2003.
- Wang XJ, Dolan PT, Dang Y, Zheng YH. Biochemical differentiation of APOBEC3F and APOBEC3G proteins associated with HIV-1 life cycle. *J Biol Chem* 2007;**282**:1585–94.
- Haché G, Liddament MT, Harris RS. The retroviral hypermutation specificity of APOBEC3F and APOBEC3G is governed by the C-terminal DNA cytosine deaminase domain. *J Biol Chem* 2005;**280**:10920–4.
- Navarro F, Bollman B, Chen H, König R, Yu Q, Chiles K, et al. Complementary function of the two catalytic domains of APOBEC3G. *Virology* 2005;**333**:374–86.
- Chen KM, Harjes E, Gross PJ, Fahmy A, Lu Y, Shindo K, et al. Structure of the DNA deaminase domain of the HIV-1 restriction factor APOBEC3G. *Nature* 2008;**452**:116–9.
- Holden LG, Prochnow C, Chang YP, Bransteitter R, Chelico L, Sen U, et al. Crystal structure of the anti-viral APOBEC3G catalytic domain and functional implications. *Nature* 2008;**456**:121–4.
- Furukawa A, Nagata T, Matsugami A, Habu Y, Sugiyama R, Hayashi F, et al. Structure, interaction and real-time monitoring of the enzymatic reaction of wild-type APOBEC3G. *EMBO J* 2009;**28**:440–51.
- Compton AA, Hirsch VM, Emerman M. The host restriction factor APOBEC3G and retroviral Vif protein coevolve due to ongoing genetic conflict. *Cell Host Microbe* 2012;**11**:91–8.
- Huthoff H, Malim MH. Identification of amino acid residues in APOBEC3G required for regulation by human immunodeficiency virus type 1 Vif and Virion encapsidation. *J Virol* 2007;**81**:3807–15.
- Huthoff H, Autore F, Gallois-Montbrun S, Fraternali F, Malim MH. RNA-dependent oligomerization of APOBEC3G is required for restriction of HIV-1. *PLoS Pathog* 2009;**5**:e1000330.
- Bulliard Y, Turelli P, Röhrig UF, Zoete V, Mangeat B, Michielin O, et al. Functional analysis and structural modeling of human APOBEC3G reveal the role of evolutionarily conserved elements in the inhibition of human immunodeficiency virus type 1 infection and Alu transposition. *J Virol* 2009;**83**:12611–21.
- Zhang KL, Mangeat B, Ortiz M, Zoete V, Trono D, Telenti A, et al. Model structure of human APOBEC3G. *PLoS One* 2007;**2**:e378.
- Chelico L, Prochnow C, Erie DA, Chen XS, Goodman MF. Structural model for deoxycytidine deamination mechanisms of the HIV-1 inactivation enzyme APOBEC3G. *J Biol Chem* 2010;**285**:16195–205.
- Harjes E, Gross PJ, Chen KM, Lu YJ, Shindo K, Nowarski R, et al. An extended structure of the APOBEC3G catalytic domain suggests a unique holoenzyme model. *J Mol Biol* 2009;**389**:819–32.
- Lavens D, Peelman F, Van der Heyden J, Uyttendaele I, Cateeuw D, Verhee A, et al. Definition of the interacting interfaces of APOBEC3G and HIV-1 Vif using MAPPIT mutagenesis analysis. *Nucl Acids Res* 2010;**38**:1902–12.
- Guo YY, Dong LY, Qiu XL, Wang YS, Zhang BL, Liu HN, et al. Structural basis for hijacking CBF- β and CUL5 E3 ligase complex by HIV-1 Vif. *Nature* 2014;**505**:229–33.
- Siu KK, Sultana A, Azimi FC, Lee JE. Structural determinants of HIV-1 Vif susceptibility and DNA binding in APOBEC3F. *Nat Commun* 2013;**4**:2593.
- Li M, Shandilya SM, Carpenter MA, Rathore A, Brown WL, Perkins AL, et al. First-in-class small molecule inhibitors of the single-strand DNA cytosine deaminase APOBEC3G. *ACS Chem Biol* 2012;**7**:506–17.
- Chen R, Li L, Weng ZP. ZDOCK: an initial-stage protein-docking algorithm. *Proteins* 2003;**52**:80–7.
- Mehle A, Wilson H, Zhang CS, Brazier AJ, McPike M, Pery E, et al. Identification of an APOBEC3G binding site in human immunodeficiency virus type 1 Vif and inhibitors of Vif–APOBEC3G binding. *J Virol* 2007;**81**:13235–41.
- Russell RA, Pathak VK. Identification of two distinct human immunodeficiency virus type 1 Vif determinants critical for interactions with human APOBEC3G and APOBEC3F. *J Virol* 2007;**81**:8201–10.
- He ZW, Zhang WY, Chen GY, Xu RZ, Yu XF. Characterization of conserved motifs in HIV-1 Vif required for APOBEC3G and APOBEC3F interaction. *J Mol Biol* 2008;**381**:1000–11.
- Tina KG, Bhadra R, Srinivasan N. PIC: protein interactions calculator. *Nucl Acids Res* 2007;**35**:W473–6.
- Cen S, Guo F, Niu MJ, Saadatmand J, Deflassieux J, Kleiman L. The interaction between HIV-1 Gag and APOBEC3G. *J Biol Chem* 2004;**279**:33177–84.
- Hu K, Clément JF, Abrahamyan L, Strelak K, Bouvier M, Kleiman L, et al. A human immunodeficiency virus type 1 protease biosensor assay using bioluminescence resonance energy transfer. *J Virol Methods* 2005;**128**:93–103.
- Cen S, Peng ZG, Li XY, Li ZR, Ma J, Wang YM, et al. Small molecular compounds inhibit HIV-1 replication through specifically stabilizing APOBEC3G. *J Biol Chem* 2010;**285**:16546–52.
- Jäger S, Kim DY, Hultquist JF, Shindo K, LaRue RS, Kwon E, et al. Vif hijacks CBF- β to degrade APOBEC3G and promote HIV-1 infection. *Nature* 2012;**481**:371–5.
- Yu YK, Xiao ZX, Ehrlich ES, Yu XH, Yu XF. Selective assembly of HIV-1 Vif-Cul5-ElonginB-ElonginC E3 ubiquitin ligase complex through a novel SOCS box and upstream cysteines. *Genes Dev* 2004;**18**:2867–72.
- Mehle A, Goncalves J, Santa-Marta M, McPike M, Gabuzda D. Phosphorylation of a novel SOCS-box regulates assembly of the HIV-1

- Vif-Cul5 complex that promotes APOBEC3G degradation. *Genes Dev* 2004;**18**:2861–6.
38. Mehle A, Thomas ER, Rajendran KS, Gabuzda D. A zinc-binding region in Vif binds Cul5 and determines cullin selection. *J Biol Chem* 2006;**281**:17259–65.
 39. Yu XH, Yu YK, Liu BD, Luo K, Kong W, Mao PY, et al. Induction of APOBEC3G ubiquitination and degradation by an HIV-1 Vif-Cul5-SCF complex. *Science* 2003;**302**:1056–60.
 40. Luo K, Xiao ZX, Ehrlich E, Yu YK, Liu BD, Zheng S, et al. Primate lentiviral virion infectivity factors are substrate receptors that assemble with cullin 5-E3 ligase through a HCCH motif to suppress APOBEC3G. *Proc Natl Acad Sci USA* 2005;**102**:11444–9.
 41. Santa-Marta M, Da Silva FA, Fonseca AM, Goncalves J. HIV-1 Vif can directly inhibit apolipoprotein B mRNA-editing enzyme catalytic polypeptide-like 3G-mediated cytidine deamination by using a single amino acid interaction and without protein degradation. *J Biol Chem* 2005;**280**:8765–75.
 42. Barraud P, Paillart JC, Marquet R, Tisne C. Advances in the structural understanding of Vif proteins. *Curr HIV Res* 2008;**6**:91–9.
 43. Wichroski MJ, Robb GB, Rana TM. Human retroviral host restriction factors APOBEC3G and APOBEC3F localize to mRNA processing bodies. *PLoS Pathog* 2006;**2**:e41.
 44. Bennett RP, Presnyak V, Wedekind JE, Smith HC. Nuclear exclusion of the HIV-1 host defense factor APOBEC3G requires a novel cytoplasmic retention signal and is not dependent on RNA binding. *J Biol Chem* 2008;**283**:7320–7.
 45. Stenglein MD, Matsuo H, Harris RS. Two regions within the amino-terminal half of APOBEC3G cooperate to determine cytoplasmic localization. *J Virol* 2008;**82**:9591–9.
 46. Shirakawa K, Takaori-Kondo A, Yokoyama M, Izumi T, Matsui M, Io K, et al. Phosphorylation of APOBEC3G by protein kinase A regulates its interaction with HIV-1 Vif. *Nat Struct Mol Biol* 2008;**15**:1184–91.
 47. Gooch BD, Cullen BR. Functional domain organization of human APOBEC3G. *Virology* 2008;**379**:118–24.